

Supporting Information

Enhancing TADF Emission and Mitigating Efficiency Roll-Off in OLEDs via Reasonable Tetrahydroquinoxaline-Integrated Organo-Boron Based Emitters

*Hongwei Xie, Mengke Li, Zhizhi Li, Zijian Chen, Zihai Yang, Kunkun Liu, and Shi-Jian Su**

State Key Laboratory of Luminescent Materials and Devices and Guangdong Basic Research Center of Excellence for Energy & Information Polymer Materials, South China University of Technology, Wushan Road 381, Tianhe District, Guangzhou 510640, P. R. China. E-mail: mssjsu@scut.edu.cn

1. General information

^1H NMR and ^{13}C NMR spectra were tested on Bruker NMR spectrometer operating at 500 or 400 MHz and 126 MHz or 101 MHz, respectively, with tetramethyl silane (TMS) as the internal standard. The samples were dissolved in deuterated chloroform (CDCl_3) or methylene chloride (CD_2Cl_2) solvent and measured at room temperature. MALDI-TOF mass spectrometry was conducted on a Waters SYNAPT G2-Si mass spectrometer. The HOMO energy levels were obtained from photoelectron yield measurement (AC-3) of the neat films, and the LUMO energy level can be calculated by the on-set of the ultra-violet to visible (UV-vis) absorption spectra. UV-vis absorption spectra were measured using Perkin-Elmer Lambda 950-PKA, while photoluminescence (PL) spectra were recorded by FluoroMax-4 spectrofluorometer (Horiba Jobin Yvon), respectively. Photoluminescence quantum yields (PLQYs) of doped films were measured utilizing an integrating sphere of Hamamatsu absolute PLQY spectrometer (C11347-11). Transient PL decay was evaluated by Edinburgh FLS980 fluorescence spectrophotometer equipped with Oxford Instruments nitrogen cryostat (Optistat DN).

2. Quantum chemical method

All of the simulations were performed using the Gaussian 09 E01 program package.^[1] Ground state (S_0) geometries were initially optimized using the B3LYP functional with 6-31g(d) basis set in vacuum according to density functional theory (DFT). All the excited states were optimized based on S_0 geometries using time-dependent density functional theory (TD-DFT) under B3LYP/6-31g(d) theoretical level in toluene with polarizable continuum model (PCM). The distribution of HOMO and LUMO were analyzed by using Multiwfn.^[2] The Huang-Rhys factors (HRf) were determined with the DUSHIN module in MOMAP (Molecular Materials Property Prediction Package).^[3] The corresponding spin-orbital coupling (SOC) matrix elements were calculated based on the optimized geometries by using the spin-orbit mean-field (SOMF) approaches in ORCA.^[4,5]

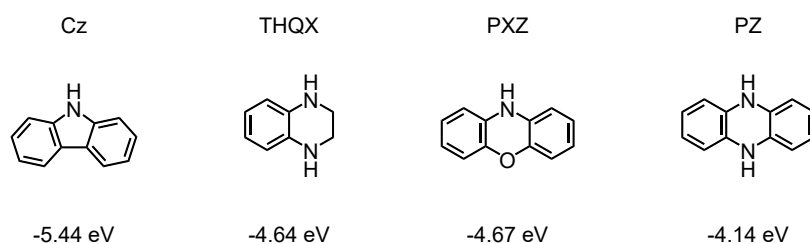


Figure S1. HOMO energy levels of different donor units.

3. Estimation for the rate constants.

Rate constants for the titled compounds in 1 wt% doped PhCzBCz films at room temperature are determined from the measurements of quantum yields and lifetimes of the prompt fluorescence (PF) and delayed fluorescence (DF) components according to equations 1-7.

$$k_r^S = \frac{\Phi_{PF}}{\tau_{PF}}$$

Equation (1) :

$$\Phi_{PL} = \frac{k_r^S}{k_r^S + k_{nr}^S}$$

Equation (2) :

$$\Phi_{PF} = \frac{k_r^S}{k_r^S + k_{nr}^S + k_{ISC}}$$

Equation (3) :

$$k_{PF} = \frac{1}{\tau_{PF}}$$

Equation (4) :

$$k_{DF} = \frac{1}{\tau_{DF}}$$

Equation (5) :

$$k_{ISC} = \frac{(1 - \Phi_{PF}) \cdot k_r^S}{\Phi_{PF}}$$

Equation (6) :

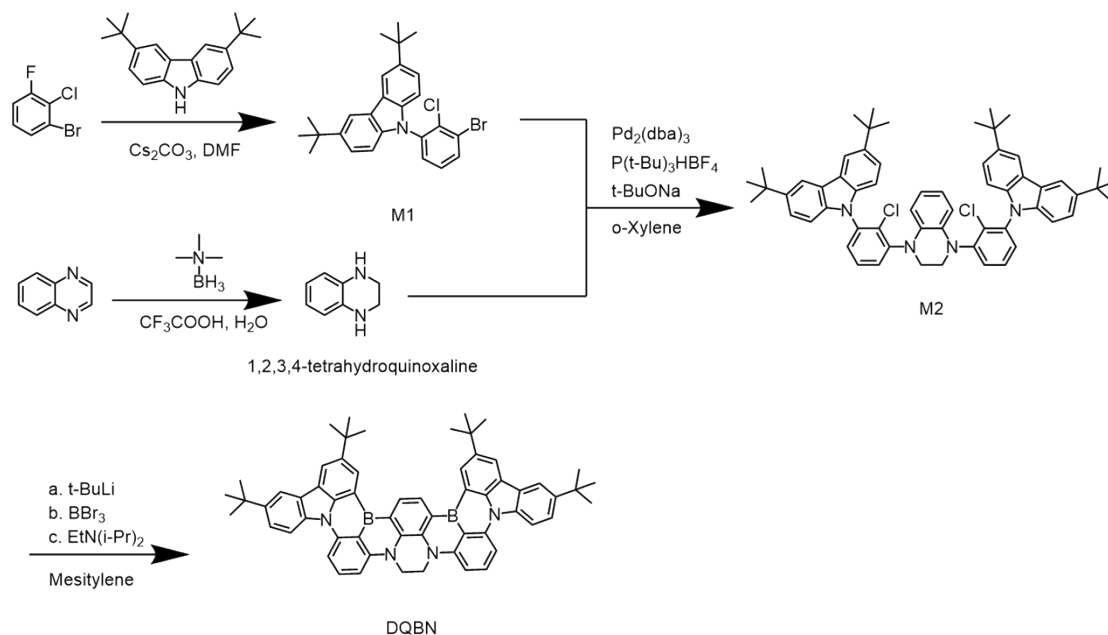
$$k_{RISC} = \frac{k_{PF} \cdot k_{DF} \cdot \Phi_{DF}}{k_{ISC} \cdot \Phi_{PF}}$$

Equation (7) :

4. Device fabrication and characterization

All the organic materials for device fabrication were available from p-OLED, Xi'an Polymer Light Technology Corp. Glass substrates pre-coated with a 95-nm-thin layer of indium tin oxide (ITO) with a sheet resistance of 10Ω per square were thoroughly cleaned in ultrasonic bath of tetrahydrofuran, isopropyl alcohol, detergent, deionized water, and isopropyl alcohol and treated with O_2 plasma for 10 min in sequence. Organic layers were deposited onto the ITO-coated glass substrates by thermal evaporation under high vacuum ($\sim 10^{-5}$ Pa). Cathode was patterned using a shadow mask with an array of $3 \text{ mm} \times 3 \text{ mm}$ openings. Deposition rates are $1 - 2 \text{ \AA s}^{-1}$ for organic materials, 0.1 \AA s^{-1} for LiF, and 6 \AA s^{-1} for aluminum, respectively. Electroluminescence (EL) spectra were recorded by Photo Research PR745. The current density and luminance versus driving voltage characteristics were measured by Keithley 2420 and Konica Minolta chromameter CS-200. External quantum efficiencies (EQEs) were calculated from the current density, luminance, and EL spectra, assuming a Lambertian distribution.

5. Synthesis and structural characterization of materials



Scheme S1. Synthetic routes for **DQBN**.

Synthesis of 9-(3-bromo-2-chlorophenyl)-3,6-di-*tert*-butyl-9H-carbazole (M1).

A mixture of 1-bromo-2-chloro-3-fluorobenzene (10.00 g, 47.75 mmol), 3,6-di-*tert*-butyl-9H-carbazole (13.34 g, 47.75 mmol) and Cs_2CO_3 (17.11 g, 52.52 mmol) were added to anhydrous *N,N*-dimethylformamide (DMF, 50 mL) under nitrogen atmosphere. The reaction was refluxed overnight and then cooled to room temperature. The mixture was extracted with dichloromethane and water for three times. The organic phase was concentrated under reduced pressure. The crude product was washed with ethanol to afford white solids (19.0 g, yield of 85%). ^1H NMR (400 MHz, Chloroform-*d*) δ = 8.14 (d, $J=2.0$, 2H), 7.80 (dd, $J=8.1$, 1.6, 1H), 7.44 (dd, $J=8.5$, 2.1, 3H), 7.31 (t, $J=8.0$, 1H), 6.98 (d, $J=8.6$, 2H).

Synthesis of 1,2,3,4-tetrahydroquinoxaline.

A mixture of quinoxaline (5.00 g, 38.42 mmol), trimethylamine borane (2.80 g, 38.42 mmol) were added to H_2O (300 mL) in a round bottom flask under air, and then the trifluoroacetic acid (14.71 mL, 192.09 mmol) was dropped into the mixture with a syringe at room temperature. The mixture was stirred for 3 hours in air at room temperature. After that, an appropriate amount of sodium hydroxide aqueous solution was added to adjust the PH value of the solution to neutrality.

The mixture was extracted with dichloromethane and water for three times. The organic phase was concentrated under reduced pressure. The crude product was washed with ethanol to afford pale yellow solids (5.0 g, 97%), the solid is unstable in air, so the next reaction is directly carried out without further purification. ¹H NMR (400 MHz, Chloroform-*d*) δ = 6.58 (dd, *J*=5.8, 3.4, 2H), 6.50 (dd, *J*=5.7, 3.4, 2H), 3.42 (s, 4H), 2.81 (s, 2H).

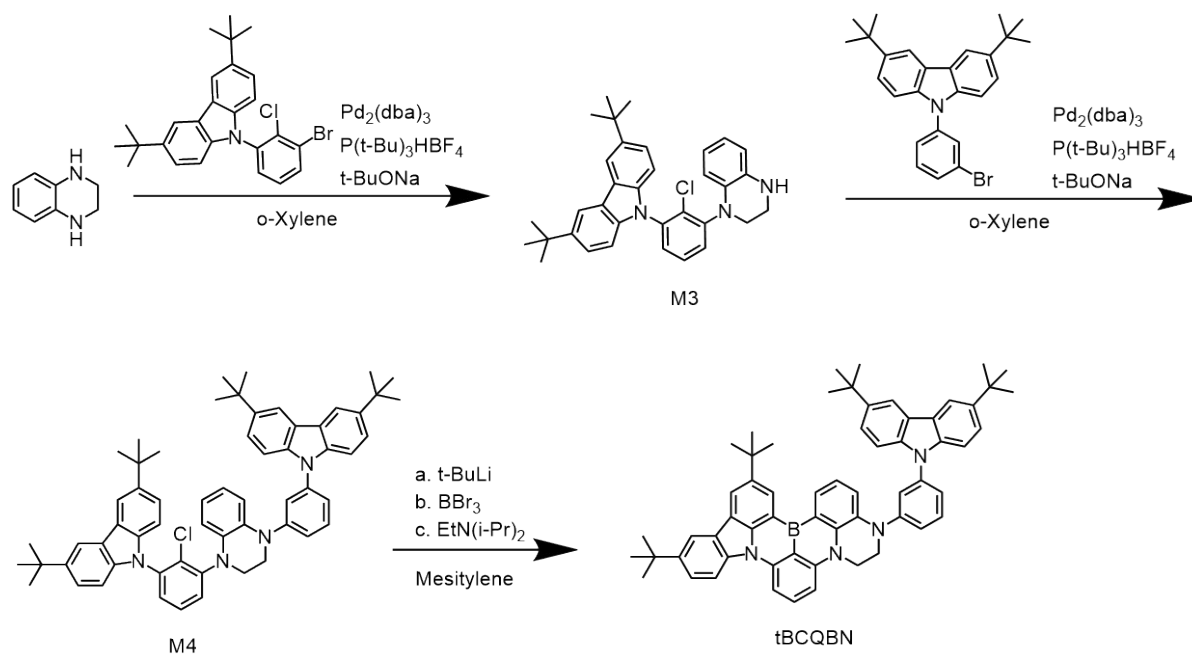
Synthesis of 1,4-bis(2-chloro-3-(3,6-di-*tert*-butyl-9H-carbazol-9-yl)phenyl)-1,2,3,4-tetrahydroquinoxaline (M2).

A mixture of 1,2,3,4-tetrahydroquinoxaline (1.50 g, 11.18 mmol), M1 (10.48 g, 22.36 mmol), Pd₂(dba)₃ (0.05 g, 0.05 mmol), P(*t*-Bu)₃HBF₄ (0.03 g, 0.11 mmol) and *t*-BuONa (2.79 g, 29.07 mmol) were added to 50 mL anhydrous *o*-xylene under nitrogen atmosphere. The reaction was refluxed overnight and then cooled to room temperature. The mixture was extracted with dichloromethane and water for three times. The organic phase was concentrated under reduced pressure and the residue was purified by chromatography on silica gel (eluent: dichloromethane/hexane = 1:4) to afford white solids (4.37 g, 43%). ¹H NMR (400 MHz, Chloroform-*d*) δ = 8.15 (d, *J*=1.9, 4H), 7.53 (d, *J*=6.2, 2H), 7.50 – 7.42 (m, 6H), 7.38 (dd, *J*=7.7, 1.7, 2H), 7.08 (d, *J*=8.6, 4H), 6.74 (dt, *J*=7.2, 3.6, 2H), 6.57 (dd, *J*=6.0, 3.5, 2H), 3.87 (s, 4H), 1.47 (s, 36H).

Synthesis of DQBN.

M2 (2.00 g, 2.20 mmol) was dissolved into 20 mL anhydrous mesitylene in a 100 mL Schlenk tube. The gas in the tube is replaced by nitrogen for three times. The mixture was added *t*-BuLi (1.3 M, 6.76 mL) dropwise under nitrogen atmosphere at -40 °C. After stirring for 15 minutes, the reaction mixture was heated at 80 °C for 3 hours. Then the reaction mixture was cooled to -30 °C, and boron tribromide (BBr₃) (0.85 mL, 8.79 mmol) was added, followed by stirring at room temperature for 3 hours. Then the reaction mixture was cooled to 0 °C, and *N,N*-diisopropylethylamine (EtN(*i*-Pr)₂) (3.06 mL) was added, followed by stirring at 160 °C for 12 hours. After cooling to room temperature, the reaction mixture was quenched by water and extracted with dichloromethane and water for three times, After the solvent was removed under reduced pressure, the residue was purified by chromatography on silica gel (eluent: ethyl acetate/hexane=1/40) to afford orange solids (0.57 g, 30%). ¹H NMR (500 MHz, Chloroform-*d*) δ = 8.99 (d, *J*=1.8, 2H), 8.76 (s, 2H), 8.45 (d, *J*=1.8, 2H), 8.28 (d, *J*=2.1, 2H), 8.18 (d, *J*=8.8, 2H),

7.86 (d, $J=8.2$, 2H), 7.63 – 7.56 (m, 4H), 7.07 (d, $J=8.4$, 2H), 4.47 (s, 4H), 1.71 (s, 18H), 1.55 (s, 18H). ^{13}C NMR (126 MHz, CDCl_3) δ 144.99, 144.95, 144.59, 142.68, 141.63, 138.13, 134.37, 132.67, 129.72, 127.03, 126.29, 125.93, 124.13, 123.39, 121.67, 121.15, 119.63, 117.01, 114.10, 104.85, 44.73, 35.26, 34.79, 32.40, 31.89. MALDI-TOF mass: calculated for $\text{C}_{60}\text{H}_{58}\text{B}_2\text{N}_4$ $[\text{M}]^+$ 856.48, found 856.0703.



Scheme S2. Synthetic routes for tBCQBN.

Synthesis of 3,6-di-*tert*-butyl-9-(2-chloro-3-(3,4-dihydroquinoxalin-1(2H)-yl)phenyl)-9H-carbazole (M3).

A mixture of 1,2,3,4-tetrahydroquinoxaline (2.00 g, 14.93 mmol), M1 (5.00 g, 10.66 mmol), $\text{Pd}_2(\text{dba})_3$ (0.10 g, 0.11 mmol), $\text{P}(\text{t-Bu})_3\text{HBF}_4$ (0.06 g, 0.21 mmol) and t-BuONa (1.54 g, 16.00 mmol) were added to 50 mL anhydrous *o*-xylene under nitrogen atmosphere. The reaction was refluxed overnight and then cooled to room temperature. The mixture was extracted with dichloromethane and water for three times. The organic phase was concentrated under reduced pressure and the residue was purified by chromatography on silica gel (eluent: dichloromethane/hexane = 1:2) to afford white solids (3.65 g, 65%). ^1H NMR (500 MHz, Chloroform- d) δ = 8.16 (d, $J=2.0$, 2H), 7.49 – 7.38 (m, 4H), 7.33 (dd, $J=7.7$, 1.8, 1H), 7.06 (d, $J=8.6$, 2H), 6.72 – 6.65 (m, 1H), 6.66 – 6.54 (m, 2H), 6.43 (d, $J=9.3$, 1H), 3.73 (s, 2H), 3.50 (s, 2H), 2.97 (s, 1H), 1.46 (s, 18H).

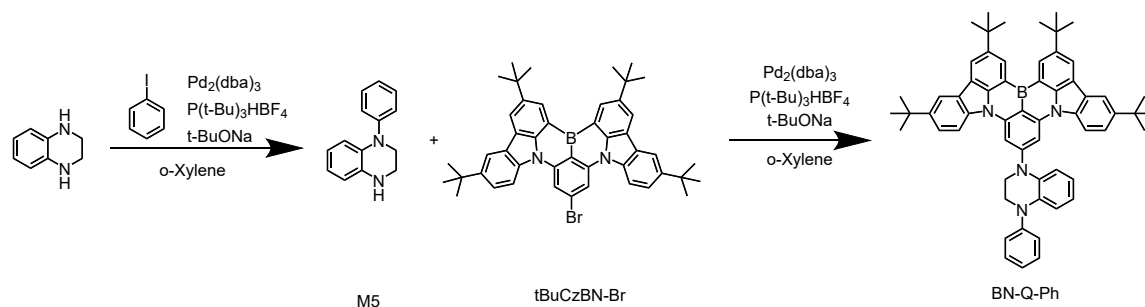
Synthesis of 3,6-di-*tert*-butyl-9-(3-(4-(2-chloro-3-(3,6-di-*tert*-butyl-9H-carbazol-9-yl)phenyl)-3,4-dihydroquinoxalin-1(2H)-yl)phenyl)-9H-carbazole (M4).

A mixture of M3 (1.30 g, 2.49 mmol), 9-(3-bromophenyl)-3,6-di-*tert*-butyl-9H-carbazole (1.08 g, 2.49 mmol), Pd₂(dba)₃ (0.05 g, 0.05 mmol), P(*t*-Bu)₃HBF₄ (0.03 g, 0.10 mmol) and *t*-BuONa (0.48 g, 4.97 mmol) were added to 40 mL anhydrous *o*-xylene under nitrogen atmosphere. The reaction was refluxed overnight and then cooled to room temperature. The mixture was extracted with dichloromethane and water for three times. The organic phase was concentrated under reduced pressure and the residue was purified by chromatography on silica gel (eluent: dichloromethane/hexane = 1:3) to afford white solids (1.54 g, 71%). ¹H NMR (400 MHz, Chloroform-*d*) δ = 8.13 (dd, *J*=9.8, 1.9, 4H), 7.57–7.38 (m, 11H), 7.31 (s, 1H), 7.22 (d, *J*=8.0, 1H), 7.15 (dd, *J*=7.8, 1.7, 1H), 7.06 (d, *J*=8.6, 2H), 6.75 (dtd, *J*=22.1, 7.4, 1.6, 2H), 6.51 (dd, *J*=7.9, 1.6, 1H), 3.90 (t, *J*=4.6, 2H), 3.80 (s, 2H), 1.46 (d, *J*=2.6, 36H).

Synthesis of tBCQBN.

M4 (1.54 g, 1.76 mmol) was dissolved into 20 mL anhydrous mesitylene in a 100 mL Schlenk tube. The gas in the tube is replaced by nitrogen for three times. The mixture was added *t*-BuLi (1.3 M, 2.71 mL) dropwise under nitrogen atmosphere at -40 °C. After stirring for 15 minutes, the reaction mixture was heated at 80 °C for 3 hours. Then the reaction mixture was cooled to -30 °C, and boron tribromide (BBr₃) (0.34 mL, 3.52 mmol) was added, followed by stirring at room temperature for 3 hours. Then the reaction mixture was cooled to 0 °C, and *N,N*-diisopropylethylamine (EtN(*i*-Pr)₂) (1.23 mL) was added, followed by stirring at 160 °C for 12 hours. After cooling to room temperature, the reaction mixture was quenched by water and extracted with dichloromethane and water for three times. After the solvent was removed under reduced pressure, the residue was purified by chromatography on silica gel (eluent: ethyl acetate/hexane=1/50) to afford yellow solids (0.30 g, 20%). ¹H NMR (400 MHz, Methylene Chloride-*d*₂) δ = 8.82 (d, *J*=1.9, 1H), 8.47 (dd, *J*=7.7, 1.5, 1H), 8.38 (d, *J*=1.8, 1H), 8.30 (d, *J*=8.8, 1H), 8.21 (d, *J*=2.1, 1H), 8.11–8.03 (m, 3H), 7.88 (t, *J*=8.3, 1H), 7.59 (dd, *J*=8.8, 2.1, 1H), 7.52 (t, *J*=8.0, 1H), 7.48–7.35 (m, 6H), 7.28 (dd, *J*=8.0, 2.3, 1H), 7.24–7.14 (m, 3H), 4.42 (t, *J*=5.3, 2H), 4.02 (t, *J*=5.3, 2H), 1.54 (s, 7H), 1.44 (s, 13H), 1.37 (s, 16H). ¹³C NMR (101 MHz, CDCl₃) δ 148.43, 145.88, 145.07, 142.96, 139.50, 139.04, 138.24, 135.75, 133.77, 133.10, 130.59, 129.67, 129.14, 127.08, 124.16, 123.67, 123.45, 120.66, 120.34, 120.24, 119.70, 117.13, 116.28, 114.00, 109.32,

105.09, 48.14, 46.36, 35.20, 34.75, 32.28, 32.03, 31.86. MALDI-TOF mass: calculated for $C_{60}H_{61}BN_4 [M]^+$ 848.50, found 848.0848.



Scheme S3. Synthetic routes for BN-Q-Ph.

Synthesis of 1-phenyl-1,2,3,4-tetrahydroquinoline (M5).

A mixture of 1,2,3,4-tetrahydroquinoline (2.21 g, 16.47 mmol), iodobenzene (1.85 mL, 16.47 mmol), $Pd_2(dba)_3$ (0.15 g, 0.16 mmol), $P(t-Bu)_3HBF_4$ (0.10 g, 0.33 mol) and $t-BuONa$ (1.90 g, 19.76 mmol) were added to 60 mL anhydrous *o*-xylene under nitrogen atmosphere. The reaction was refluxed overnight and then cooled to room temperature. The mixture was extracted with dichloromethane and water for three times. The organic phase was concentrated under reduced pressure and the residue was purified by chromatography on silica gel (eluent: dichloromethane/hexane = 1:3) to afford white solids (2.14 g, 62%). 1H NMR (400 MHz, Methylene Chloride- d_2) δ = 7.35 – 7.27 (m, 2H), 7.23 – 7.16 (m, 2H), 7.02 (t, $J=7.3$, 1H), 6.83 (dd, $J=8.0$, 1.4, 1H), 6.70 (t, $J=7.5$, 1H), 6.64 – 6.44 (m, 2H), 3.70 (s, 2H), 3.44 (s, 2H), 2.69 (s, 1H).

Synthesis of tBuCzBN-Br.

The synthesis process was referred to the reported literature [6].

Synthesis of BN-Q-Ph.

A mixture of tBuCzBN-Br (2.00 g, 2.78 mmol), M5 (0.70 g, 3.34 mmol), $Pd_2(dba)_3$ (0.13 g, 0.14 mmol), $P(t-Bu)_3HBF_4$ (0.08 g, 0.18 mmol) and $t-BuONa$ (0.53 g, 5.56 mmol) were added to 60 mL anhydrous *o*-xylene under nitrogen atmosphere. The reaction was refluxed overnight and then cooled to room temperature. The mixture was extracted with dichloromethane and water for three times. The organic phase was concentrated under reduced pressure and the residue was purified by chromatography on silica gel (eluent: dichloromethane/hexane = 1:6) to afford brown solids (1.46 g, 62%). 1H NMR (500 MHz, Chloroform- d) δ = 9.10 (d, $J=1.9$, 2H), 8.43 (d, $J=1.8$, 2H), 8.25 (d, $J=2.1$, 2H), 8.21 – 8.14 (m, 4H), 7.73 – 7.68 (m, 1H), 7.57 (dd, $J=8.7$, 2.1, 2H), 7.43

– 7.35 (m, 4H), 7.20 – 7.15 (m, 1H), 7.05 – 7.01 (m, 1H), 7.00 – 6.95 (m, 2H), 4.22 (dd, $J=5.8, 4.0$, 2H), 3.91 – 3.86 (m, 2H), 1.67 (s, 18H), 1.51 (s, 18H). ^{13}C NMR (101 MHz, CDCl_3) δ 145.34, 145.25, 144.60, 141.83, 138.15, 131.45, 129.74, 129.62, 127.13, 124.65, 124.33, 123.44, 122.64, 120.85, 120.22, 117.28, 113.85, 101.12, 50.04, 48.39, 35.17, 34.79, 32.21, 31.83. MALDI-TOF mass: calculated for $\text{C}_{60}\text{H}_{61}\text{BN}_4$ $[\text{M}]^+$ 848.99, found 847.9704.

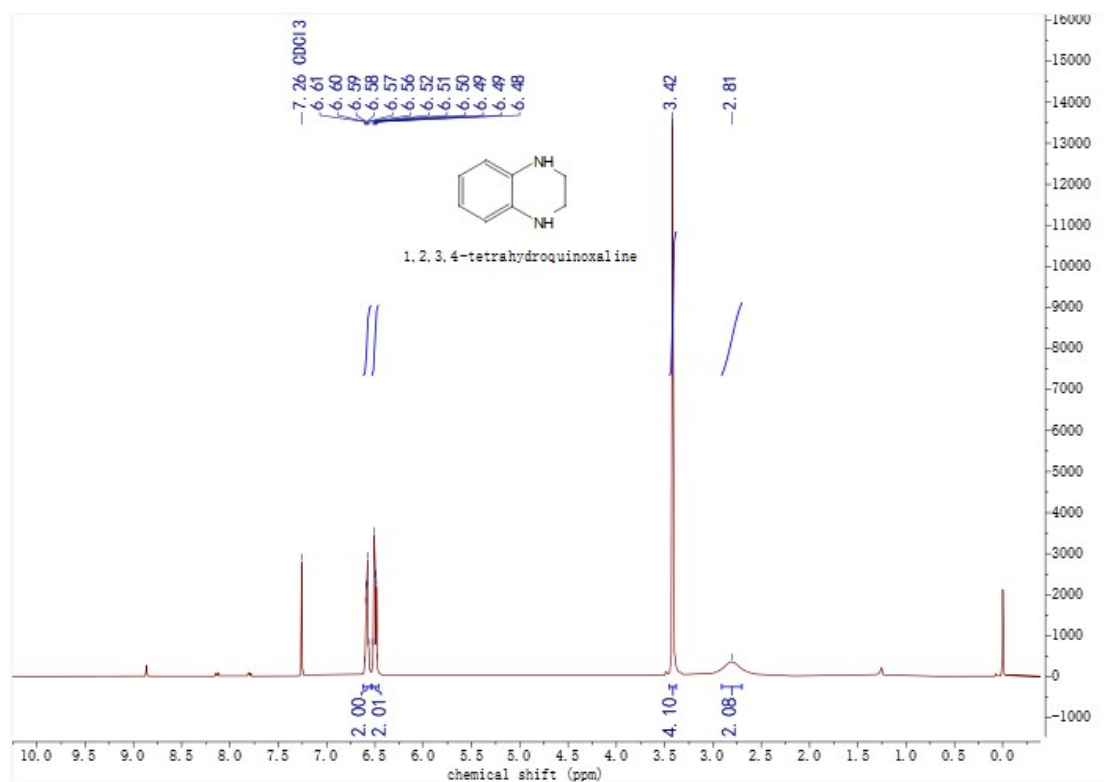
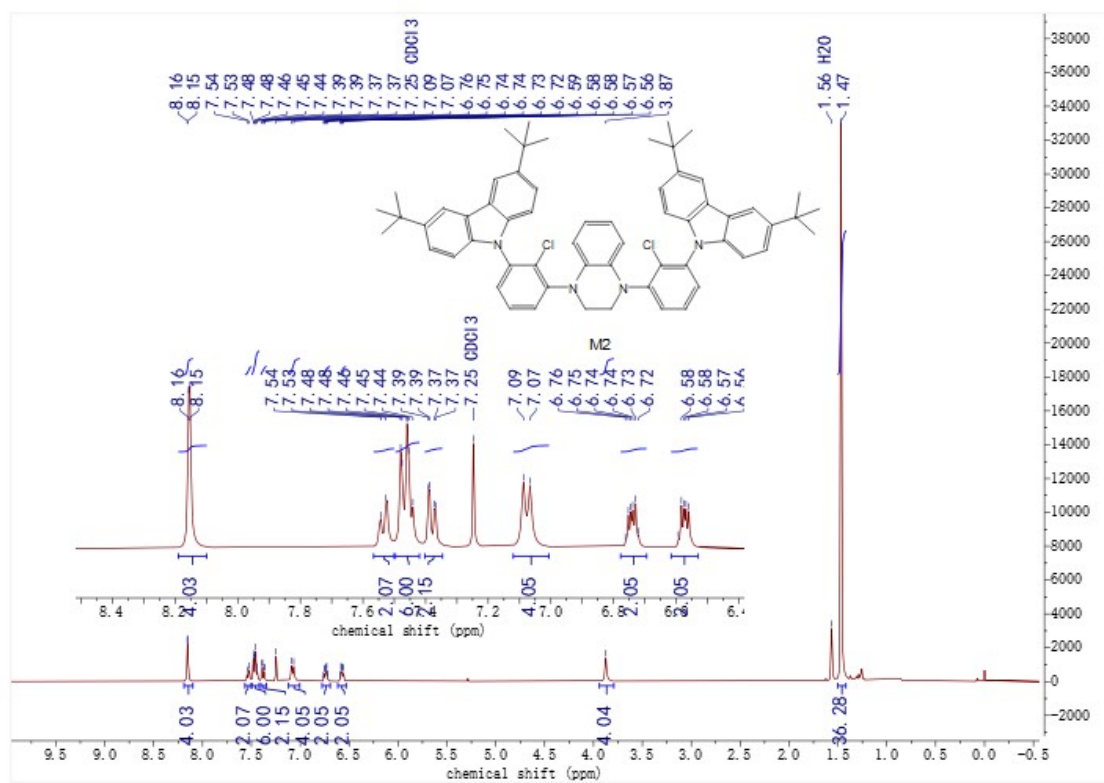
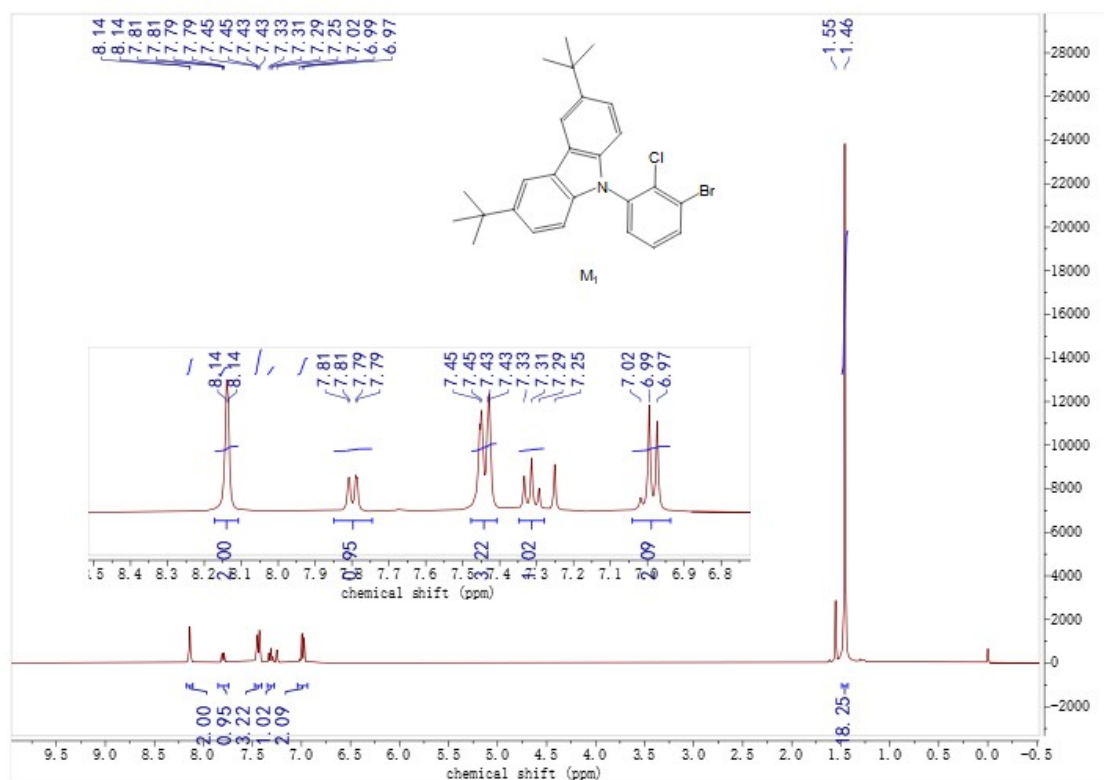


Figure S2. ^1H NMR spectrum of compound **1,2,3,4-tetrahydroquinoxaline**. (400 MHz, CDCl_3)



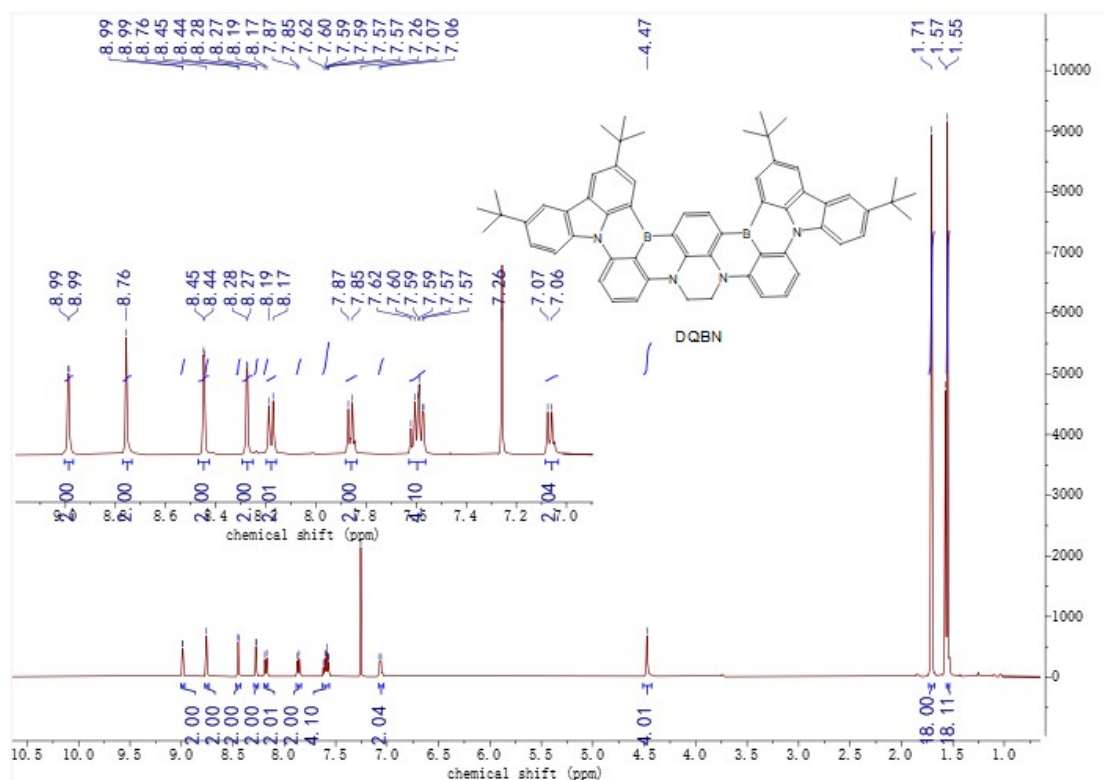


Figure S5. ¹H NMR spectrum of compound DQBN. (500 MHz, CDCl₃)

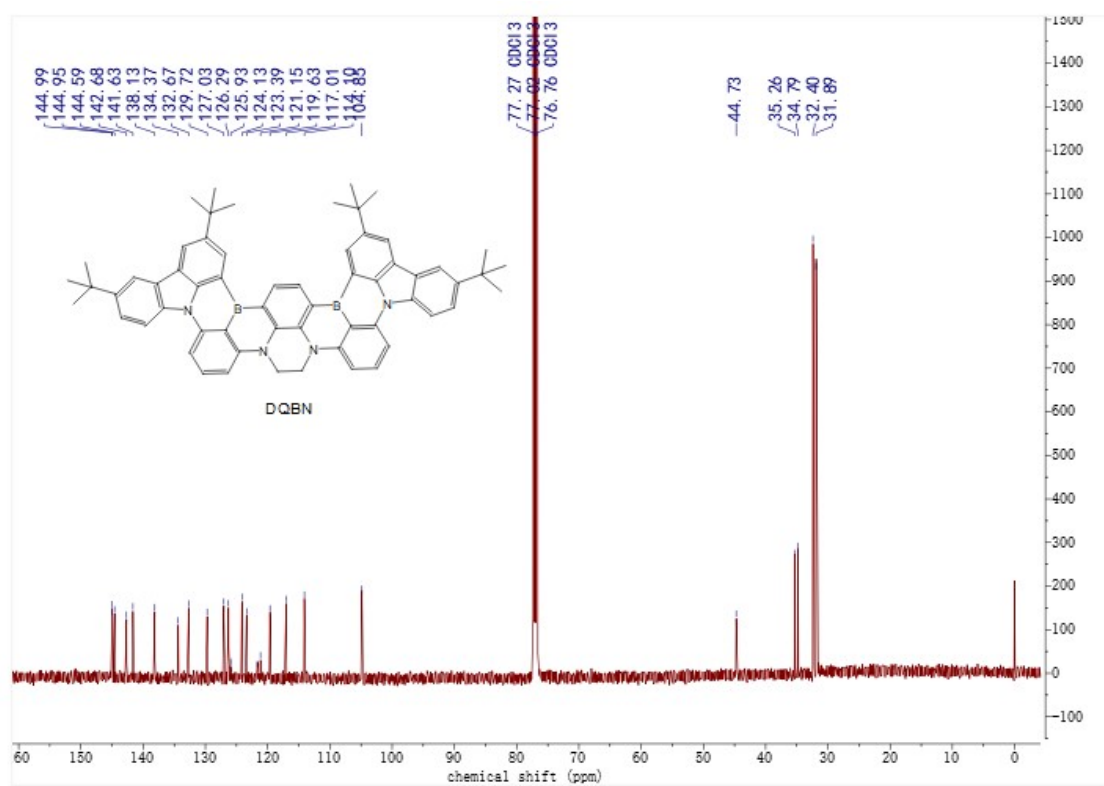


Figure S6. ¹³C NMR spectrum of compound DQBN. (126 MHz, CDCl₃)

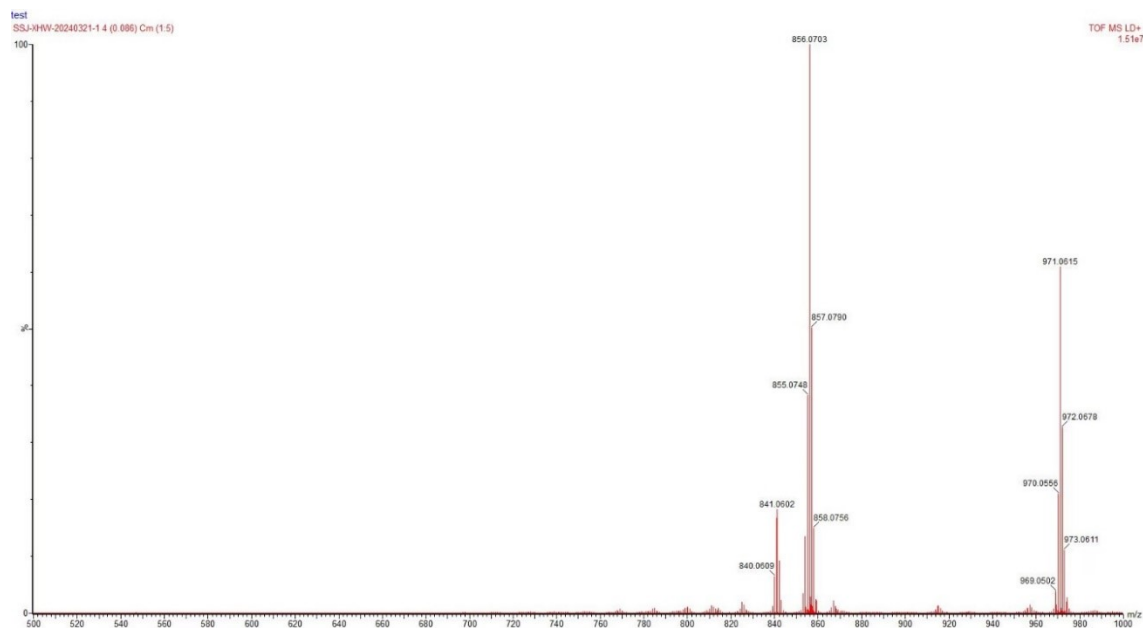


Figure S7. MALDI-TOF mass spectrum of compound **DQBN**.

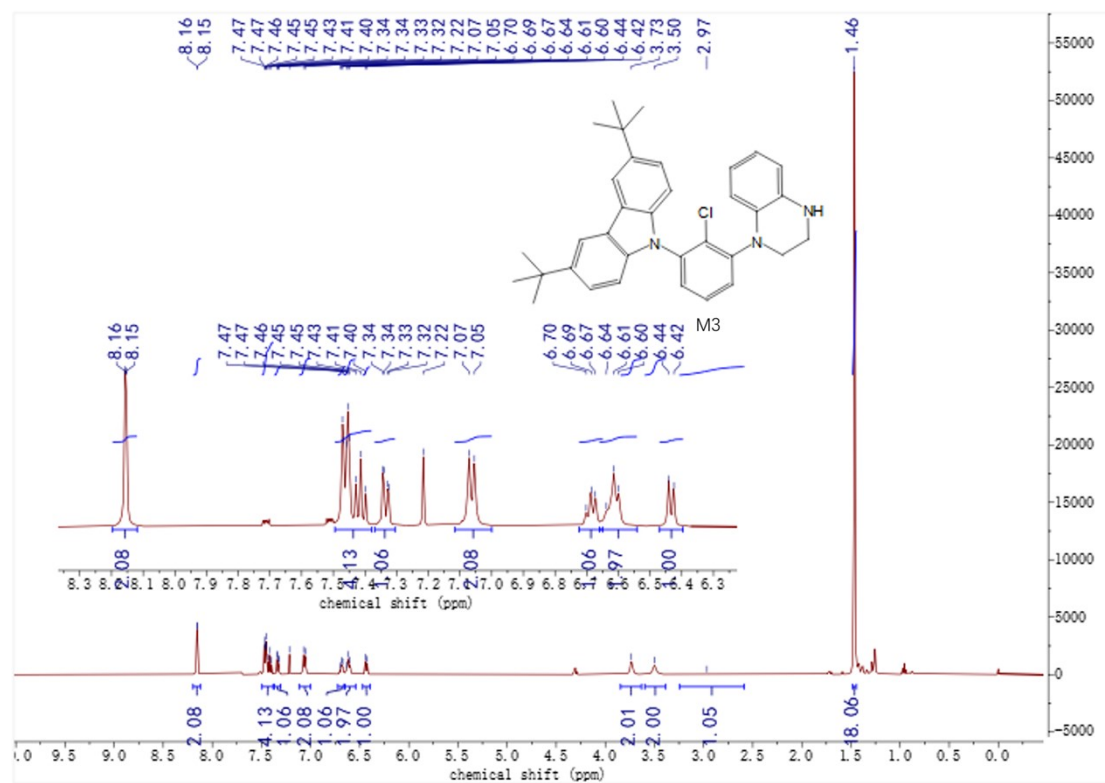


Figure S8. ^1H NMR spectrum of compound **M3**. (500 MHz, CDCl_3)

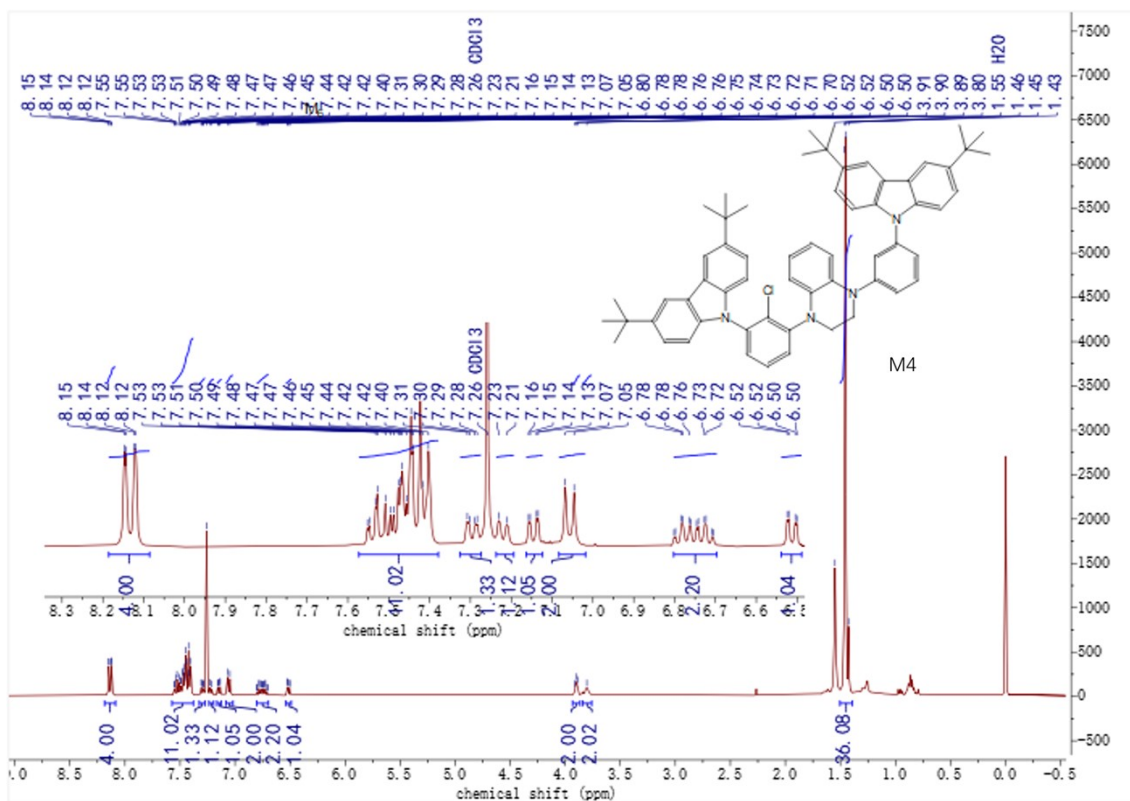


Figure S9. ^1H NMR spectrum of compound **M4**. (400 MHz, CDCl_3)

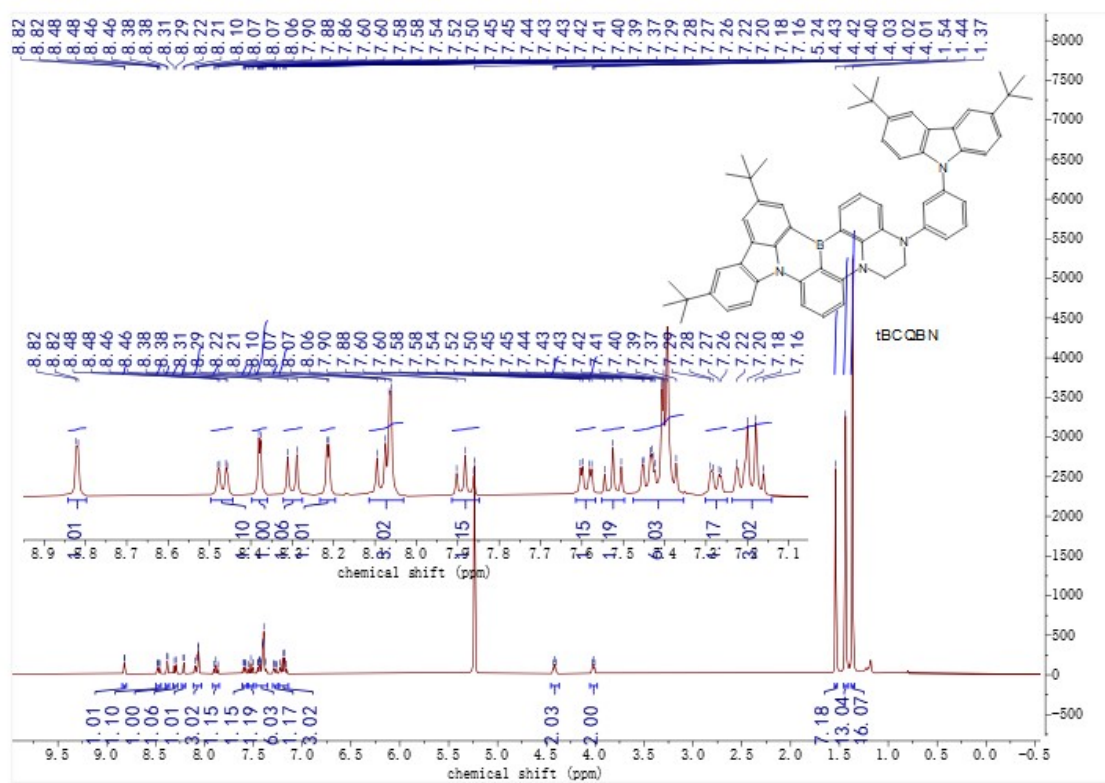


Figure S10. ^1H NMR spectrum of compound **tBCQBN**. (400 MHz, CDCl_3)

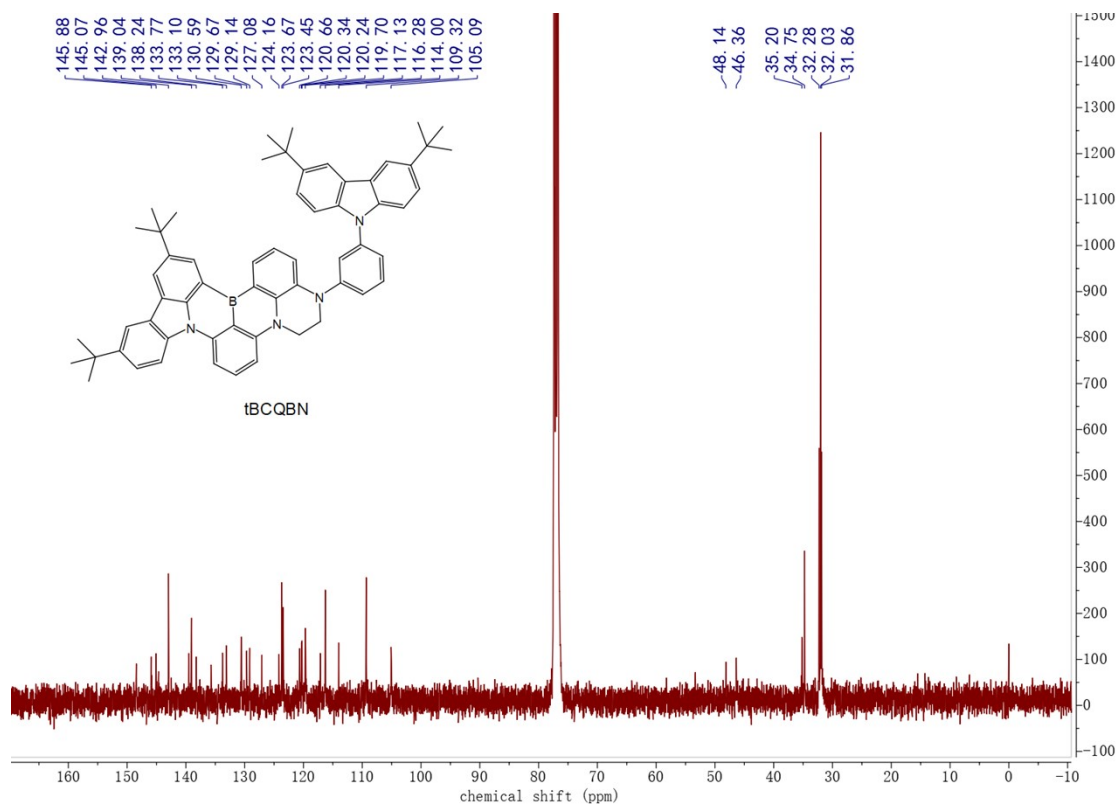


Figure S11. ^{13}C NMR spectrum of compound **tBCQBN**. (101 MHz, CDCl_3)

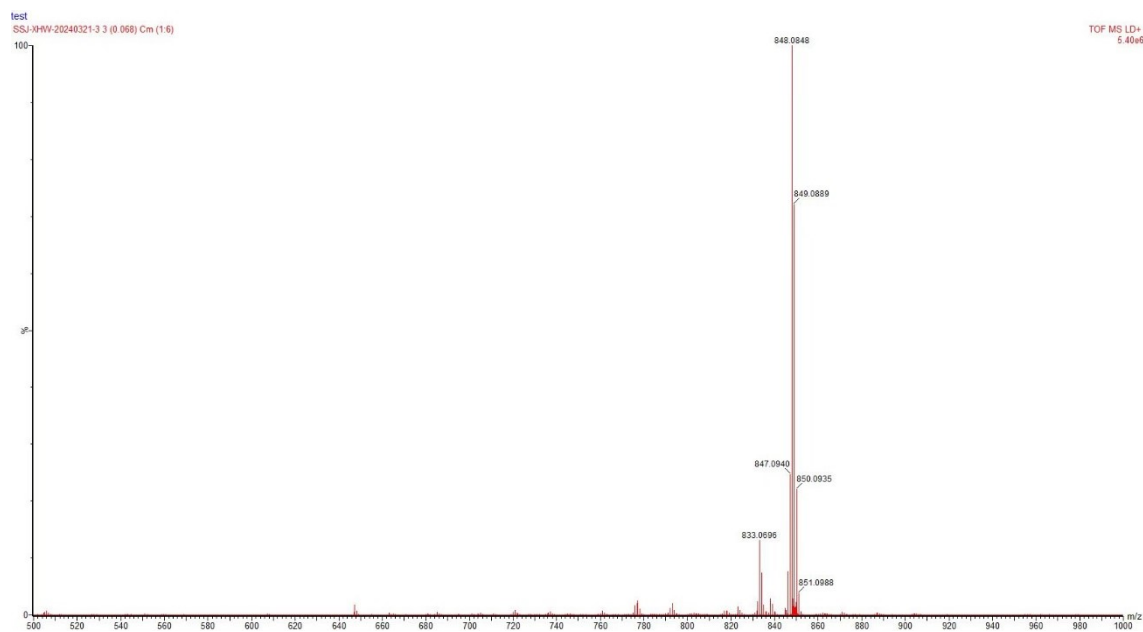


Figure S12. MALDI-TOF mass spectrum of compound **tBCQBN**.

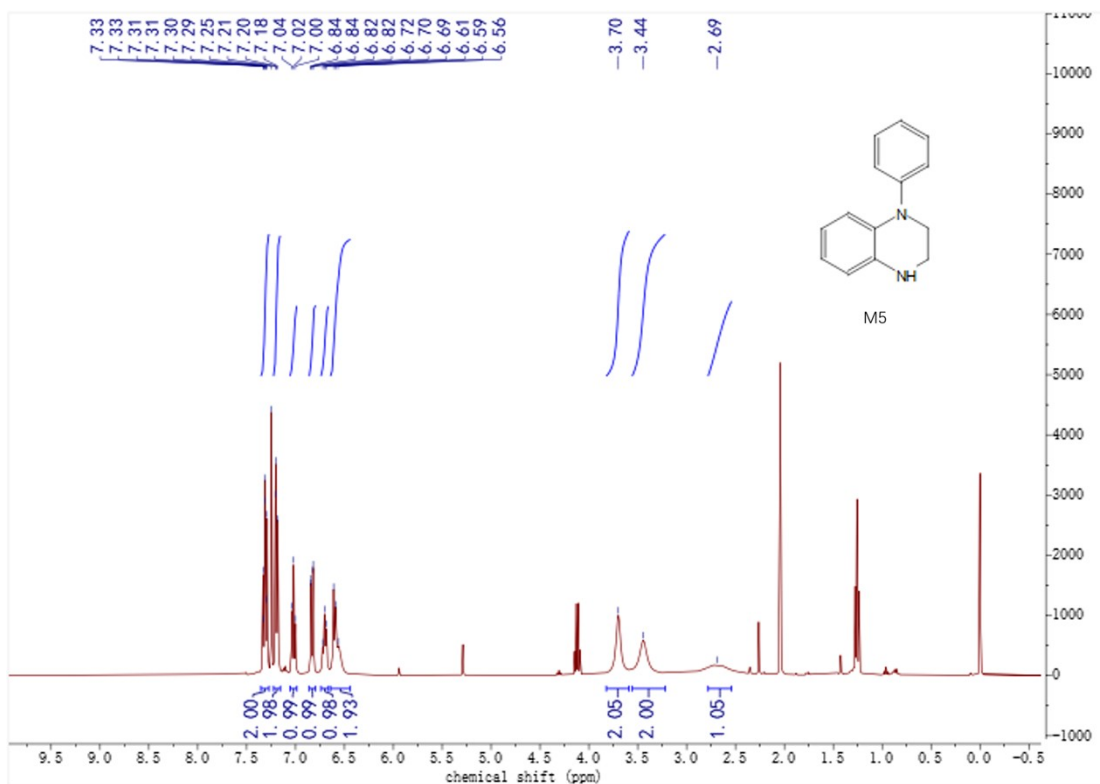


Figure S13. ^1H NMR spectrum of compound M5. (400 MHz, CD_2Cl_2)

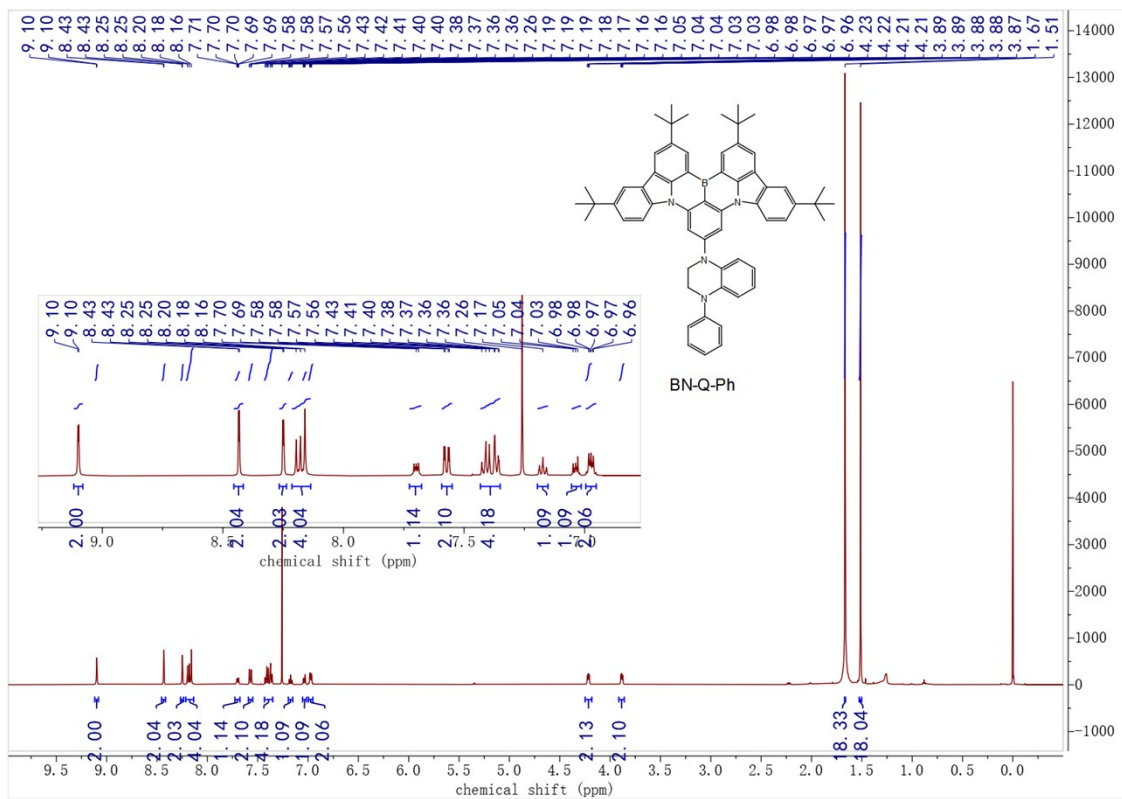


Figure S14. ^1H NMR spectrum of compound BN-Q-Ph. (500 MHz, CDCl_3)

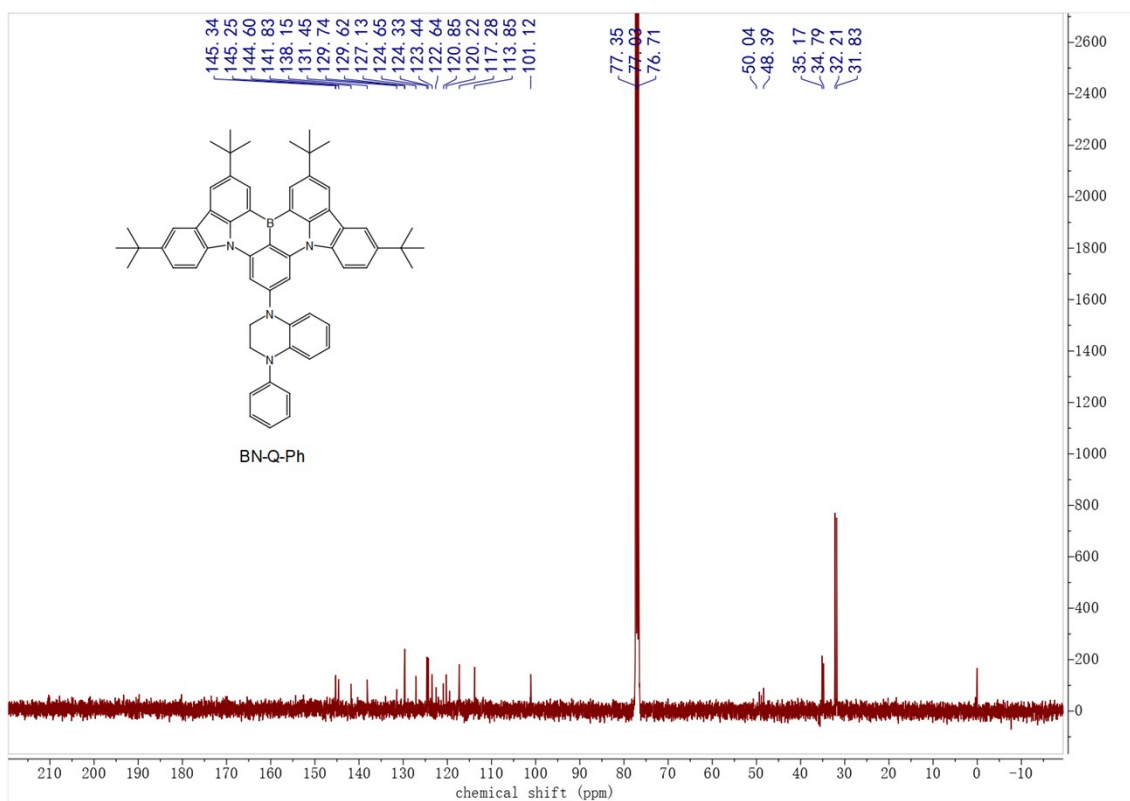


Figure S15. ^{13}C NMR spectrum of compound **BN-Q-Ph**. (101 MHz, CDCl_3)

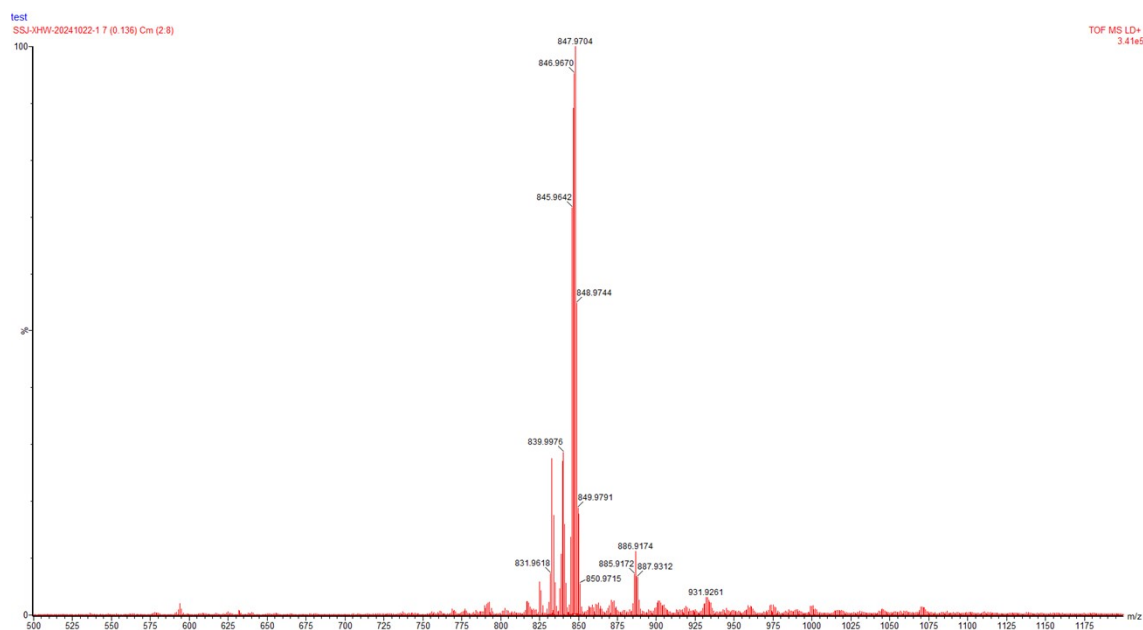


Figure S16. MALDI-TOF mass spectrum of compound **BN-Q-Ph**.

6. Supplementary figures and tables

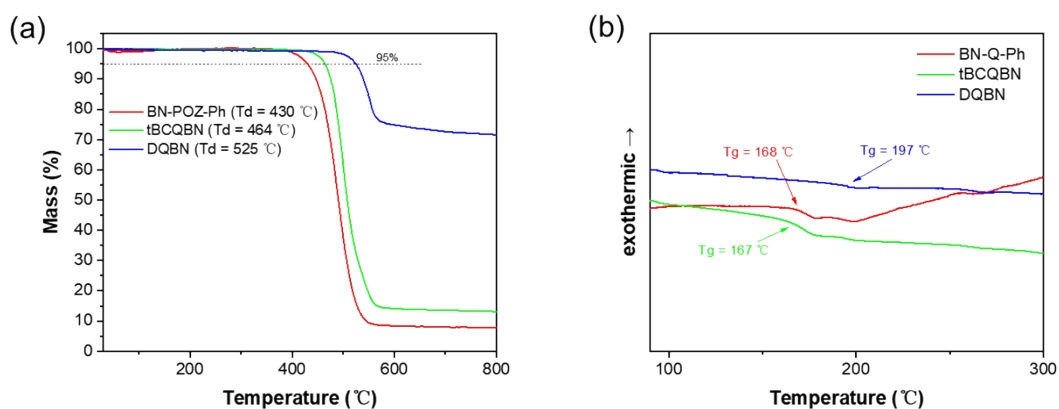


Figure S17. a) Thermal gravimetric analysis (TGA) curves and b) differential scanning calorimetry (DSC) analysis curves of the investigated compounds.

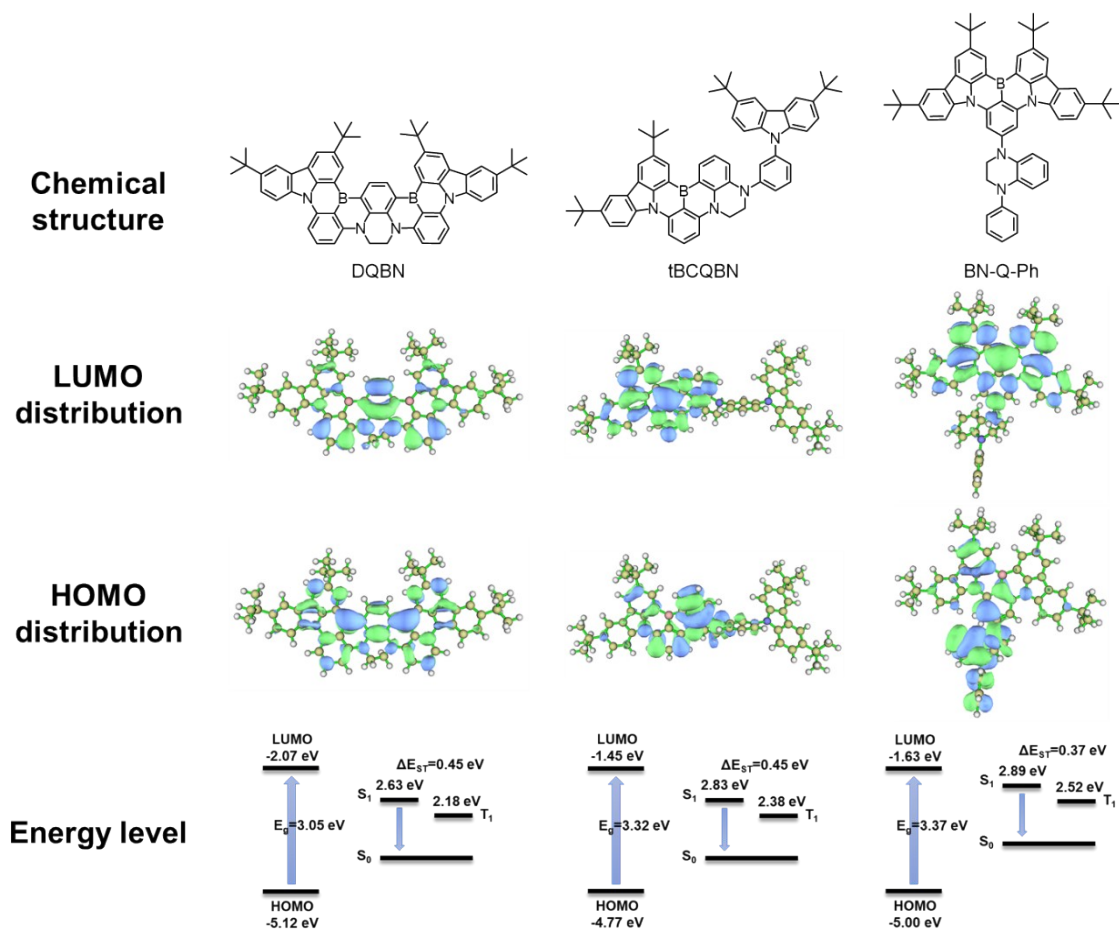


Figure S18. Chemical structures, HOMO/LUMO distributions and calculated energy levels of DQBN, tBCQBN and BN-Q-Ph.

Table S1. Summary of the calculated energy level data and oscillator strengths of DQBN, tBCQBN and BN-Q-Ph.

Emitters	LUMO [eV]	HOMO [eV]	E_g [eV]	S_1 [eV]	f/S_1	S_2 [eV]	f/S_2	T_1 [eV]	ΔE_{ST} [eV]
DQBN	-2.07	-5.12	3.05	2.63	0.09	2.84	0.59	2.18	0.45
tBCQBN	-1.45	-4.77	3.32	2.83	0.27	3.26	0.14	2.38	0.45
BN-Q-Ph	-1.63	-5.00	3.37	2.89	0.34	2.98	0.17	2.52	0.37

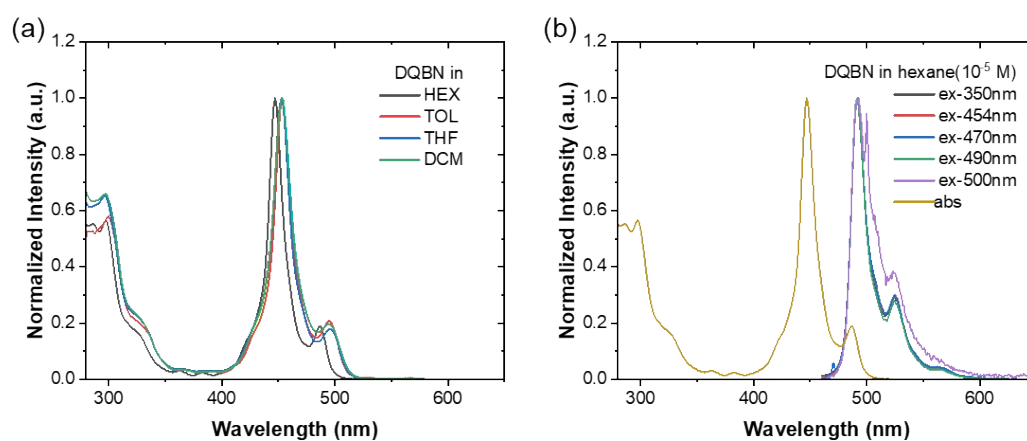


Figure S19. a) UV-vis absorption spectra of DQBN in different polar solvents. b) PL spectra at different excitation wavelengths and UV-vis absorption spectra of DQBN in dilute hexane solution.

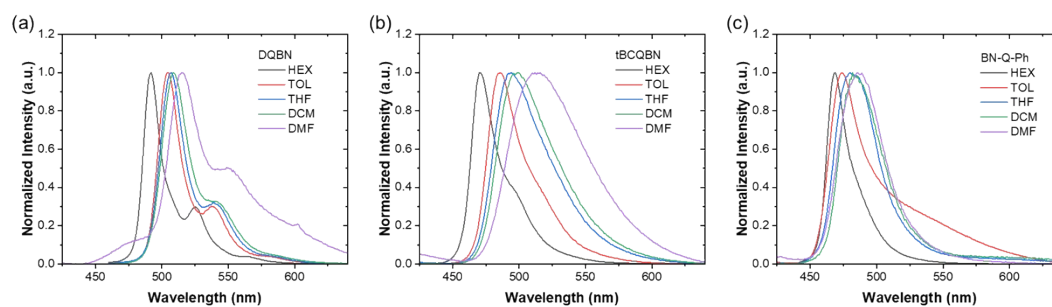


Figure S20. PL spectra of a) DQBN, b) tBCQBN and c) BN-Q-Ph in different polar solvents.

Table S2. Summary of the emission peak wavelengths and FWHMs of DQBN, tBCQBN and BN-Q-Ph in different polar solvents.

	DQBN		tBCQBN		BN-Q-Ph	
	Peak (nm)	FWHM (nm)	Peak (nm)	FWHM (nm)	Peak (nm)	FWHM (nm)
Hexane	492	16	470	24	469	21
Toluene	504	20	484	33	474	33
Tetrahydrofuran	507	22	494	48	480	37
Dichloromethane	509	25	499	51	483	37
N, N-dimethylformamide	515	35	513	68	487	39

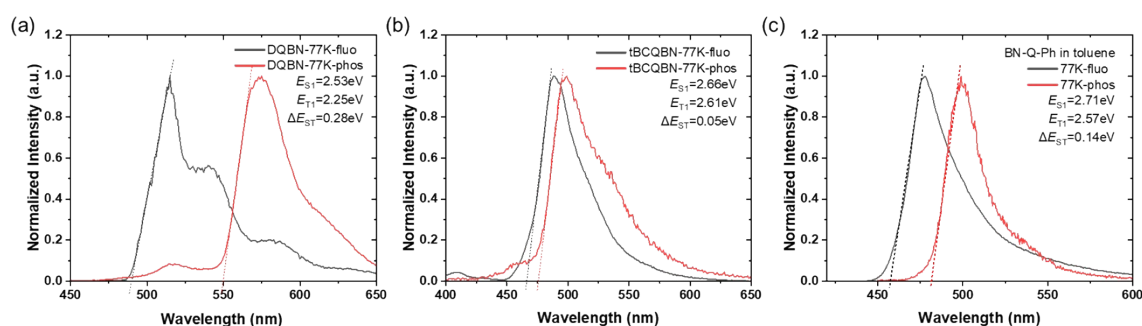


Figure S21. Fluorescence and phosphorescence spectra of a) DQBN, b) tBCQBN and c) BN-Q-Ph in solution at 77K.

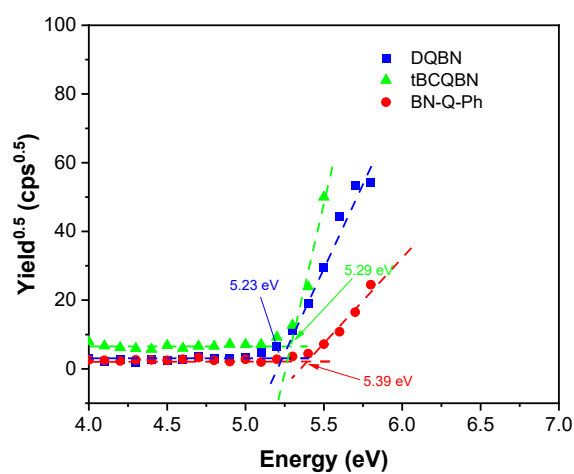


Figure S22. Atmospheric ultraviolet photoelectron spectroscopies of DQBN, tBCQBN and BN-Q-Ph.

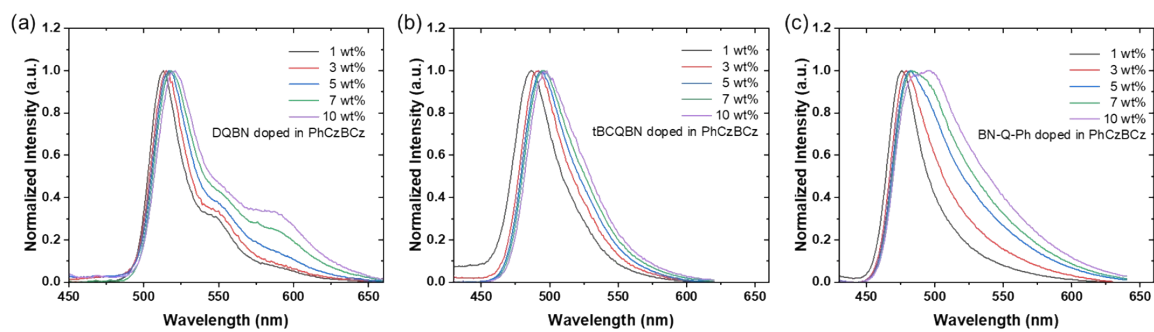


Figure S23. PL spectra of a) DQBN, b) tBCQBN and c) BN-Q-Ph doped in PhCzBCz film at different concentrations.

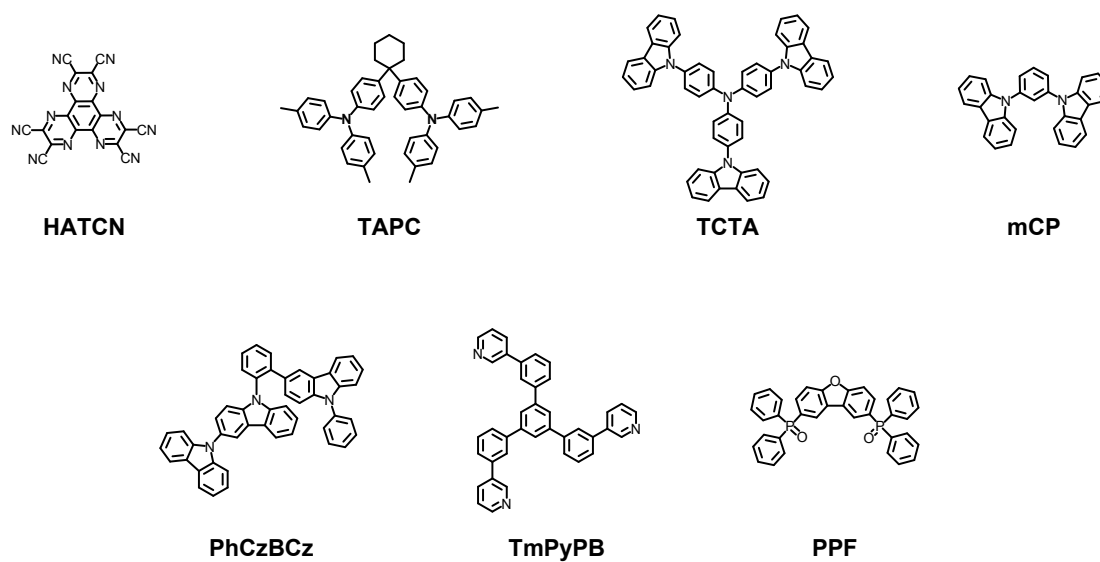


Figure S24. Chemical structures of the materials utilized in OLED devices.

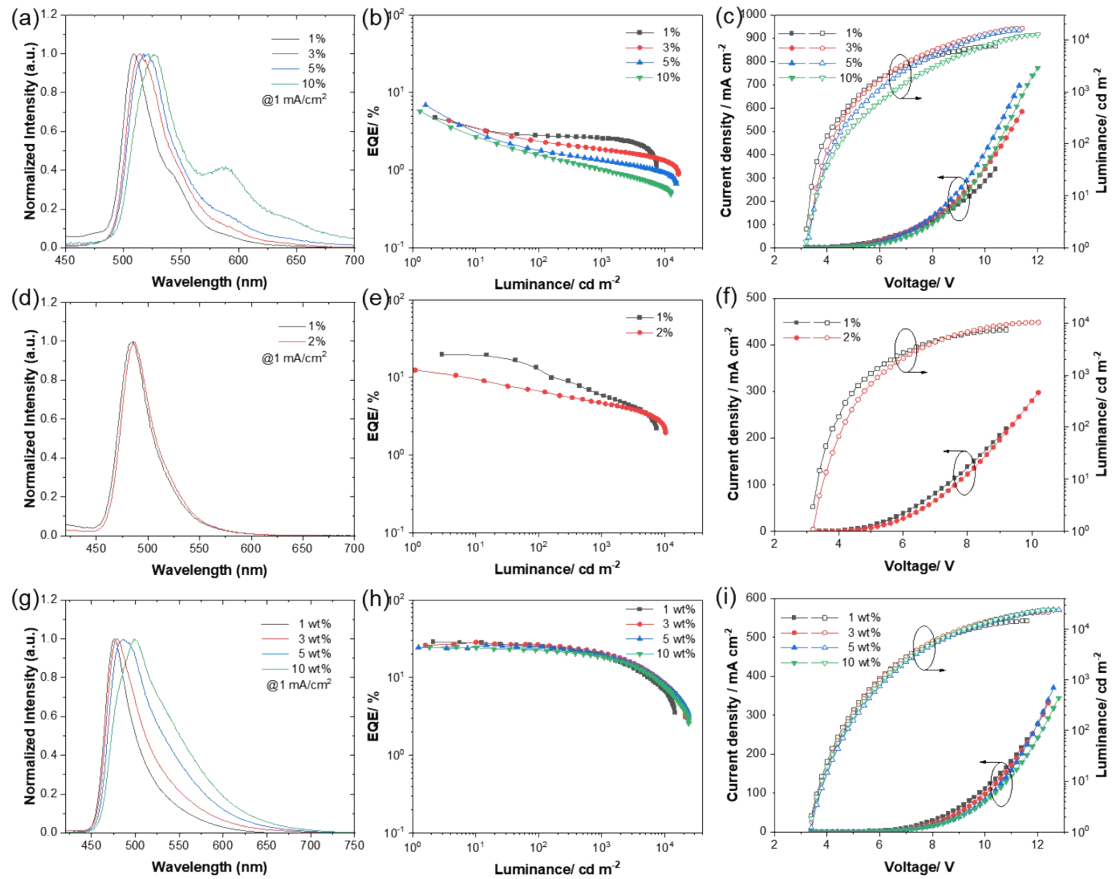


Figure S25. EL performance of the devices at different doping concentrations. a) EL spectra, b) EQE-luminance, and c) J-V-L characteristics of the devices based on DQBN as emitter. d) EL spectra, e) EQE-luminance, and f) J-V-L characteristics of the devices based on tBCQBN as emitter. g) EL spectra, h) EQE-luminance, and i) J-V-L characteristics of the devices based on BN-Q-Ph as emitter.

Table S3. Summary of EL properties of the devices based on DQBN, tBCQBN and BN-Q-Ph as emitter in various doping concentrations.

devices	Doped concentrations	$\lambda_{\text{EL}}^{(a)}$ [nm]	FWHM ^(a) [nm]	$V_{\text{on}}^{(b)}$ [V]	$L_{\text{max}}^{(c)}$ [cd m ⁻²]	CE _{max} ^(d) [cd A ⁻¹]	PE _{max} ^(e) [lm W ⁻¹]	EQE _{max/100/1000} ^(f) [%]	CIE ^(g) [x,y]
DQBN	1 wt%	509	33	3.2	7534	12.2	11.9	4.7/2.8/2.6	[0.19,0.54]
	3 wt%	515	40	3.4	16473	14.1	13.0	4.4/2.4/1.9	[0.24,0.65]
	5 wt%	520	43	3.3	15253	18.6	17.7	6.9/1.8/1.3	[0.27,0.65]
	10 wt%	526	45	3.2	12473	16.8	16.5	5.7/1.6/1.0	[0.36,0.60]
tBCQBN	1 wt%	484	35	3.2	7437	35.2	34.5	19.8/12.6/6.0	[0.12,0.32]
	2 wt%	487	35	3.2	10278	25.2	24.7	12.4/6.7/4.7	[0.12,0.36]
BN-Q-Ph	1 wt%	476	36	3.4	14527	65.2	60.2	28.7/25.4/19.0	[0.16,0.31]
	3 wt%	479	46	3.4	21340	69.7	57.6	28.6/26.5/20.9	[0.18,0.37]
	5 wt%	487	64	3.4	23857	70.2	55.1	26.4/24.9/20.0	[0.22,0.45]
	10 wt%	500	78	3.4	24096	71.6	62.4	24.9/22.7/18.4	[0.26,0.51]

^{a)} EL peak and FWHM at the current density of 1 mA cm⁻²; ^{b)} Turn-on voltage at the luminance of 1 cd m⁻²; ^{c)} Maximum luminance; ^{d)} Current efficiency; ^{e)} Power efficiency; ^{f)} EQE value at maximum, 100 cd m⁻² and 1000 cd m⁻², respectively; ^{g)} Commission International de L'Eclairage (CIE) coordinates at the current density of 1 mA cm⁻².

7. Reference

- [1] Gaussian 09, Revision E.01, Frisch, M. J. G. W. Trucks, H. B. Schlegel, G. E. Scuseria, M. A. Robb, J. R. Cheeseman, G. Scalmani, V. Barone, B. Mennucci, G. A. Petersson, H. Nakatsuji, M. Caricato, X. Li, H. P. Hratchian, A. F. Izmaylov, J. Bloino, G. Zheng, J. L. Sonnenberg, M. Hada, M. Ehara, K. Toyota, R. Fukuda, J. Hasegawa, M. Ishida, T. Nakajima, Y. Honda, O. Kitao, H. Nakai, T. Vreven, J. A. Montgomery, Jr., J. E. Peralta, F. Ogliaro, M. Bearpark, J. J. Heyd, E. Brothers, K. N. Kudin, V. N. Staroverov, T. Keith, R. Kobayashi, J. Normand, K. Raghavachari, A. Rendell, J. C. Burant, S. S. Iyengar, J. Tomasi, M. Cossi, N. Rega, J. M. Millam, M. Klene, J. E. Knox, J. B. Cross, V. Bakken, C. Adamo, J. Jaramillo, R. Gomperts, R. E. Stratmann, O. Yazyev, A. J. Austin, R. Cammi, C. Pomelli, J. W. Ochterski, R. L. Martin, K. Morokuma, V. G. Zakrzewski, G. A. Voth, P. Salvador, J. J. Dannenberg, S. Dapprich, A. D. Daniels, O. Farkas, J. B. Foresman, J. V. Ortiz, J. Cioslowski, and D. J. Fox, Gaussian, Inc., Wallingford CT, 2013.
- [2] M. Ma, J. Li, D. Liu, Y. Mei, R. Dong, *ACS Appl. Mater. Interfaces* **2021**, *13*, 44615-44627.
- [3] T. Hua, J. Miao, H. Xia, Z. Huang, X. Cao, N. Li, C. Yang, *Adv. Funct. Mater.* **2022**, *32*, 2201032.
- [4] F. Neese, *WIREs Comput. Mol. Sci.* **2011**, *2*, 73.
- [5] F. Neese, *WIREs Comput. Mol. Sci.* **2017**, *8*, e1327.
- [6] Z. Huang, H. Xie, J. Miao, Y. Wei, Y. Zou, T. Hua, X. Cao, C. Yang, *J. Am. Chem. Soc.* **2023**, *145*, 12550-12560.